

Tracking control of nonlinear pneumatic actuator systems using static state feedback linearization of the input–output map

Jihong Wang^a, Ülle Kotta^b, and Jia Ke^a

^a Department of Electrical Engineering and Electronics, The University of Liverpool, Liverpool, L69 3GJ, UK; jhwang@liverpool.ac.uk

^b Institute of Cybernetics, Tallinn University of Technology, Akadeemia tee 21, 12618 Tallinn, Estonia; kotta@cc.ioc.ee

Received 6 November 2006

Abstract. To achieve more accurate tracking control, a control strategy for servo pneumatic systems based on the feedback linearization theory is presented. The nonlinear pneumatic actuator system is transformed into a linear system description, with a linear input–output map by regular static state feedback and state coordinate transformation. A servo tracking controller is then developed for the system based on the linear system model. Since there exists an inverse transformation for the new coordinate system, the designed servo control is transformed back to the original state coordinates with the original input variables. Two different cases are discussed: the pneumatic cylinder is driven (1) by a single five-port proportional valve and (2) by two three-port proportional valves. At the initial stage, for the convenience of analysis, the static friction forces are ignored. They are treated as uncertainties addition to the system in the later sections. For on-line implementation, the controller is simplified to require only position and velocity state variables in its feedback. The simulation results show that the simplified controller can drive the system to achieve the required tracking accuracy.

Key words: nonlinear system, tracking control, pneumatic actuators, feedback linearization, servo control.

1. INTRODUCTION

The basic idea of feedback linearization is to transform a nonlinear system model into a linear system model. Then the well-developed linear control system design techniques can be applied to the linearized systems. This methodology has converted many previously intractable nonlinear problems into simpler solvable forms. The techniques have two main themes: the input-state linearization, where

the full state equation is linearized, and the input–output linearization, where the map from input to output is emphasized even if the state equations are only partially linearizable (see [1,2]). The feedback linearization method has been used to solve a number of nonlinear control problems, but many engineers still think that it is quite naive for practical applications. This is mainly due to the exact feedback cancellation, which is very difficult or almost impossible to conduct in the practical world. The problem may be solved if the un-cancelled nonlinear dynamics are classified as a part of uncertainties and robustness is taken into account in the controller design. In some cases, the uncertainties can be estimated using nonlinear observer and the estimated variables can be used in feedback control [3]. On the other hand, the controller, designed using the feedback linearization method, can be used as a guideline for system optimization.

Pneumatic actuators are widely employed in position and speed control applications when cheap, clean, simple, and safe operating conditions are required [4]. In recent years, low-cost microprocessors and pneumatic components became available in the market, which made it possible to adopt more sophisticated control strategies in pneumatic system control. Hence, investigations have been initiated for employing pneumatic actuators to accomplish more sophisticated motion control tasks, such as servo-controlled pneumatic systems [5–12]. A servo-controlled pneumatic actuator system is a kind of tracking control systems. Enormous difficulties encountered in servo pneumatic system control due to its inherent nonlinearities are associated with compressibility of air and complex friction distributions along the cylinders. In the authors' previous work [13], the input–output linearization method has been applied to servo-controlled pneumatic actuator systems. The system is linearized first using state transformation and static state feedback. A linear servo controller is designed initially with respect to the linear system model and is then transformed back to the nonlinear state space. For the convenience of analysis, the friction forces were ignored initially in [13]. In this paper, the influences of friction forces are considered when designing the robust feedback controller by extending the work reported in [13]. The servo controller developed in this method is very complicated for implementation. So some actions of approximation are taken to simplify the structure of the controller. The simulation study indicates that the simplified controller can drive the pneumatic actuators to follow a desired profile within the accuracy requirement.

2. PNEUMATIC SYSTEM MODEL

An analysis of the dynamic behaviour of a pneumatic system usually requires individual mathematical descriptions of dynamics of the three-component parts of the system (see [14–16]): (i) the valve, (ii) the actuator, and (iii) the load. Such an analysis has been reported in [11] and [12]. Therefore, the detailed modelling procedure is not included in this paper. The coordinate system illustrated in Fig. 1 is adopted in the paper for system modelling. Pneumatic actuators can be modelled

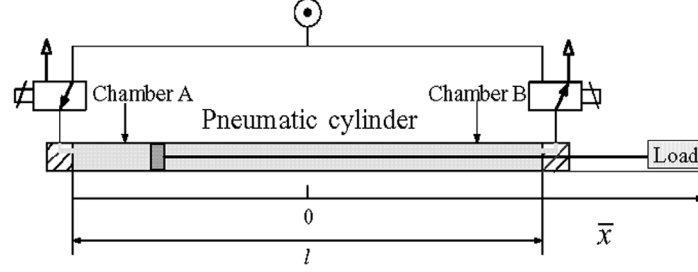


Fig. 1. Coordinate system of a pneumatic cylinder.

as a fourth-order nonlinear system affine in the control inputs [11,12]. The system equations are as follows:

$$\dot{x}_1 = x_2, \quad (1a)$$

$$\dot{x}_2 = \frac{1}{M}[-K_f x_2 - K_{S-c}(x_1)S(x_2, x_3, x_4) + A_a x_3 - A_b x_4], \quad (1b)$$

$$\dot{x}_3 = -k \left[x_3 x_2 - \frac{RT_s}{A_a} C_d C_0 w_a \hat{f}(x_3, P_s, P_e) u_1 \right] / (l/2 + x_1 + \Delta), \quad (1c)$$

$$\dot{x}_4 = k \left[x_4 x_2 + \frac{RT_s}{A_b} C_d C_0 w_b \hat{f}(x_4, P_s, P_e) u_2 \right] / (l/2 - x_1 + \Delta), \quad (1d)$$

where $x_1 = \bar{x}$, the load position (m), $x_2 = \dot{\bar{x}}$, $x_3 = P_a$, $x_4 = P_b$, $u_1 = X_a$, and $u_2 = X_b$, where subscripts a, b denote inlet and outlet chambers, respectively, P is the pressure, and $X_{a,b}$ is spool displacement of valve A or valve B (m), $K_{S-c}(x_1)$ describes a combination of static and dynamic frictions. The other symbols used in the system model are listed below:

A	Ram area (m ²)	P_e	Exhaust pressure (N/m ²)
C_d	Discharge coefficient	P_s	Supply pressure (N/m ²)
Δ	The generalized residual chamber volume	P_u	Upstream pressure (N/m ²)
K_f	Viscous frictional coefficient	R	Universal gas constant $\left(\frac{\text{J/Kg}}{\text{K}}\right)$
k	Specific heat constant	T_s	Supply temperature (K)
l	Stroke length (m) and $\bar{x} \in (-l/2, l/2)$	V	Volume (m ³)
m	Mass flow rate (Kg/s)	w	Port width (m)
M	Payload (Kg)	T_a, T_b	Temperature of chambers A and B
P_d	Downstream pressure (N/m ²)		

The following constants appear in the system model:

$$k = 1.4, \quad P_s = 6 \times 10^5 \text{ N/m}^2, \quad T_s = 293 \text{ K}, \quad C_d = 0.8,$$

$$P_e = 1 \times 10^5 \text{ N/m}^2, \quad R = 287 \frac{\text{J/Kg}}{\text{K}},$$

$$C_r = \left(\frac{2}{k+1} \right)^{k/(k-1)} = 0.528, \quad \text{and} \quad C_k = \sqrt{\frac{2}{k-1} \left(\frac{k+1}{2} \right)^{(k+1)/(k-1)}} = 3.864.$$

The functions in Eqs (1a)–(1d) are defined as

$$\tilde{f}(p_r) = \begin{cases} 1, & \frac{P_{\text{atm}}}{P_u} < p_r \leq C_r, \\ C_k [p_r^{2/k} - p_r^{(k+1)/k}]^{1/2}, & C_r < p_r < 1. \end{cases} \quad (2)$$

$$\hat{f}(x_3, P_s, P_e) = \begin{cases} P_s \tilde{f}\left(\frac{x_3}{P_s}\right) / \sqrt{T_s}, & \text{chamber A is a drive chamber,} \\ x_3 \tilde{f}\left(\frac{P_e}{x_3}\right) / \sqrt{T_a}, & \text{chamber B is a drive chamber,} \end{cases} \quad (3a)$$

and

$$\hat{f}(x_4, P_s, P_e) = \begin{cases} x_4 \tilde{f}\left(\frac{P_e}{x_4}\right) / \sqrt{T_b}, & \text{chamber A is a drive chamber,} \\ P_s \tilde{f}\left(\frac{x_4}{P_s}\right) / \sqrt{T_s}, & \text{chamber B is a drive chamber.} \end{cases} \quad (3b)$$

The term, $-K_f x_2 - K_{S-c}(x_1)S(x_2, x_3, x_4)$, in Eq. (1b) represents the summing effects of static and dynamic friction forces of the system, where

$$K_{S-c}(x_1)S(x_2, x_3, x_4) := \begin{cases} (A_a x_3 - A_b x_4), & x_2 = 0 \quad \text{and} \quad |A_a x_3 - A_b x_4| \leq K_S(x_1), \\ K_C(x_1) \text{sign}(x_2), & x_2 \neq 0 \quad \text{or} \quad |A_a x_3 - A_b x_4| > K_S(x_1), \end{cases}$$

which describes the static frictions with $x = [x_1 \quad x_2 \quad x_3 \quad x_4]^T$. In the formula, $K_S(x_1)$ represents position-dependent static frictions and $K_C(x_1)$ represents the variable position-dependent load caused by friction effects. Detailed analysis of the influences of friction forces can be found in [15]. Pneumatic system model validation was reported in [12]. For the pneumatic system, it is desired that the piston position/velocity can follow a desired trajectory or profile (for servo

control). If x_1 is chosen as a system output, that is, $y = x_1$, the tracking problem becomes an output tracking problem.

3. FEEDBACK LINEARIZATION OF THE INPUT–OUTPUT MAP

As described in the above section, the pneumatic system is modelled as a nonlinear system affine in the control inputs. The general mathematical description for such a system with a single input and single output is:

$$\begin{aligned}\dot{\hat{x}} &= f(\hat{x}) + g(\hat{x})u, \\ y &= h(\hat{x}),\end{aligned}\tag{4}$$

where $\hat{x} \in \mathfrak{R}^n$ is the state variable, $u \in \mathbb{R}$ represents the input, and $y \in \mathbb{R}$ is the system output. In (4), f and g are C^∞ vector fields on \mathfrak{R}^n and h is a C^∞ function on \mathbb{R} . The system is called static state feedback input–output linearizable by regular static state feedback and coordinate transformation if there exists an invertible feedback, i.e.

$$u = \alpha(\hat{x}) + \beta(\hat{x})v\tag{5}$$

with $\frac{\partial \beta(\hat{x})}{\partial \hat{x}} \neq 0$ and a coordinate change

$$z = \phi(\hat{x})\tag{6}$$

such that, under the z -coordinates and the new input v , system (4) becomes

$$\begin{aligned}\dot{z}^1 &= Az^1 + bv, \\ \dot{z}^2 &= f^2(z^1, z^2) + g^2(z^1, z^2)v, \\ y &= c^T z^1,\end{aligned}$$

where A, b, c are constant matrices of proper dimensions [2]. Denote by $L_f h$ the derivative of h along f , and by $L_f^k h$ the repeated derivative along f . For a single-input and single-output system, if the system has a relative degree $r \leq n$, the first r components of the local coordinate transformation can be chosen as (see [2], pp. 141–142):

$$\begin{aligned}\phi_1(\hat{x}) &= h(\hat{x}), \\ \phi_2(\hat{x}) &= L_f h(\hat{x}), \\ &\dots \\ \phi_r(\hat{x}) &= L_f^{r-1} h(\hat{x}),\end{aligned}\tag{7}$$

and it is always possible to find $n-r$ more functions $[\phi_{r+1}(\hat{x}) \phi_{r+2}(\hat{x}) \cdots \phi_n(\hat{x})]$ such that the mapping $[\phi_1(\hat{x}) \phi_{r+2}(\hat{x}) \cdots \phi_n(\hat{x})]$ qualifies as a local coordinate transformation in a neighbourhood of \hat{x}^0 (see for details [2]). Note that there is much freedom in the choice of $[\phi_{r+1}(\hat{x}) \phi_{r+2}(\hat{x}) \cdots \phi_n(\hat{x})]$, which is highly dependent on the requirements of special applications.

For a multi-input system, in Eq. (4), $u \in \mathfrak{R}^m$ represents the input, and $g(\hat{x}) = (g_1(\hat{x}) \ g_2(\hat{x}) \ \cdots \ g_m(\hat{x})) \in \mathfrak{R}^{n \times m}$. In this case, the static state feedback has the same form as shown in (5) with $\alpha(\hat{x}) \in \mathfrak{R}^m$, $\beta(\hat{x}) \in \mathfrak{R}^{m \times m}$ with $\beta(\hat{x})$ being an invertible matrix. As there is only one output in this case, the local coordinate transformation can be chosen in the same way as the one used for the case of single-input and single-output systems.

When applying the above theory to servo pneumatic actuator systems, for the convenience of analysis, the static friction forces are ignored initially and will be brought in as uncertainties in the later sections. The servo pneumatic actuators could be driven by a single five-port proportional valve or two separate three-port proportional valves. Therefore, the analysis will cover two different cases: nonlinear systems (1) with a single input and (2) with two independent inputs. The paper will discuss both cases.

Case I. System with a single five-port valve

The main purpose of the paper is to use the feedback linearization method to achieve the high-performance tracking control or servo control. When a pneumatic actuator system adopts a single five-port valve, the inlet and outlet ports are not independent inputs. The control input will be $u_1 = u$ and $u_2 = -u$ with the same port width $w_a = w_b = w$; f , g , h in (4) are as follows:

$$f(x) = \begin{bmatrix} x_2 \\ (-K_f x_2 + A_a x_3 - A_b x_4)/M \\ \frac{-kx_3 x_2}{l/2 + x_1 + \Delta} \\ \frac{-kx_4 x_2}{l/2 - x_1 + \Delta} \end{bmatrix}, \quad g(x) = \begin{bmatrix} 0 \\ 0 \\ \frac{kRT_s C_d C_0 w \hat{f}(x_3, P_s, P_e)}{A_a (l/2 + x_1 + \Delta)} \\ -\frac{kRT_s C_d C_0 w \hat{f}(x_4, P_s, P_e)}{A_b (l/2 - x_1 + \Delta)} \end{bmatrix}, \quad \text{and}$$

$$y = h(x) = x_1,$$

where f and g are C^∞ vector fields on the set $\Omega \subset \mathfrak{R}^4$ (there are some constraints on the system variables and parameters in practice), $y = h(x) \in (-l/2, l/2) \subset \mathfrak{R}$.

Since, for this system, $L_g L_f^k h(x) = 0$, for all $k < 3$ and $L_g L_f^3 h(x) \neq 0$ ($\forall x$), the relative degree of the system is 3. Using the formulae in (7), we can choose the following coordinate transformation to linearize the system:

$$\begin{aligned}
z_1 &= x_1, \\
z_2 &= x_2, \\
z_3 &= -\frac{K_f}{M}x_2 + \frac{A_a}{M}x_3 - \frac{A_b}{M}x_4, \\
z_4 &= x_4,
\end{aligned} \tag{8}$$

or in the matrix form $z = \bar{T}x$ with $\bar{T} = \begin{bmatrix} 1 & 0 & 0 & 0 \\ 0 & 1 & 0 & 0 \\ 0 & -\frac{K_f}{M} & \frac{A_a}{M} & -\frac{A_b}{M} \\ 0 & 0 & 0 & 1 \end{bmatrix}$.

Applying the transformation (8), the pneumatic system is transformed into

$$\begin{aligned}
\dot{z}_1 &= z_2, \\
\dot{z}_2 &= z_3, \\
\dot{z}_3 &= -\frac{K_f}{M}z_3 - \frac{k(z_2z_3 + K_fz_2^2/M)}{l/2 + z_1 + \Delta} - \frac{A_bk(l + 2\Delta)}{(l/2 + \Delta)^2 - z_1^2}z_2z_4 + \psi(z)u, \\
\dot{z}_4 &= \frac{kz_4z_2}{l/2 - z_1 + \Delta} - \frac{kRT_sC_dC_0w\hat{f}(z_4, P_s, P_e)}{A_b(l/2 - z_1 + \Delta)}u,
\end{aligned} \tag{9}$$

where

$$\psi(z) = kRT_sC_dC_0w \frac{(l/2 - z_1 + \Delta)\hat{f}(z, P_s, P_e) + (l/2 + z_1 + \Delta)\hat{f}(z_4, P_s, P_e)}{M[(l/2 + \Delta)^2 - z_1^2]}.$$

Let

$$u = \frac{1}{\psi(z)} \left[\frac{k(z_2z_3 + K_fz_2^2/M)}{l/2 + z_1 + \Delta} + \frac{A_bk(l + 2\Delta)z_2z_4}{(l/2 + \Delta)^2 - z_1^2} + V \right].$$

Substituting u into (9), we have

$$\begin{aligned}
\dot{z}_1 &= z_2, \\
\dot{z}_2 &= z_3, \\
\dot{z}_3 &= -\frac{K_f}{M}z_3 + V,
\end{aligned} \tag{10a}$$

and

$$\dot{z}_4 = \frac{kz_4z_2}{l/2 - z_1 + \Delta} - \eta(z) \left[\frac{k(z_2z_3 + K_f z_2^2/M)}{l/2 + z_1 + \Delta} + \frac{A_b k(l + 2\Delta)z_2z_4}{(l/2 + \Delta)^2 - z_1^2} + V \right], \quad (10b)$$

$$y = z_1, \quad (10c)$$

$$\text{where } \eta(z) = \frac{1}{\psi(z)} \frac{kRT_s C_d C_0 w_b \hat{f}(z_4, P_s, P_e)}{A_b(l/2 - z_1 + \Delta)}.$$

Subsystem (10a) is linear with respect to z and V and the input–output map of the system (10) is linear as well.

Case II. System with two three-port valves

When the pneumatic actuator adopts two three-port valves, the system has the same vector field f , and the output $h(x) = x_1$, but the matrix function g becomes

$$g(x) = \begin{bmatrix} 0 & 0 \\ 0 & 0 \\ \frac{kRT_s C_d C_0 w \hat{f}(x_3, P_s, P_e)}{A_a(l/2 + x_1 + \Delta)} & 0 \\ 0 & \frac{kRT_s C_d C_0 w \hat{f}(x_4, P_s, P_e)}{A_b(l/2 - x_1 + \Delta)} \end{bmatrix},$$

where $g \in \Omega \subset \mathfrak{R}^{4 \times 2}$. Since $L_{g_i} L_f^k h(x) = 0$ ($i=1, 2$), for all $k < 3$ and $L_{g_i} L_f^3 h(x) \neq 0$ ($i=1, 2$) ($\forall x$), the relative degree of the system is 3. The system is a multi-input and single-output system and the same transformation as in Case I can be applied in this case. Applying formulae (7), we can choose the coordinate transformation (8) again. Then, the pneumatic system is transformed into

$$\begin{aligned} \dot{z}_1 &= z_2, \\ \dot{z}_2 &= z_3, \\ \dot{z}_3 &= -\frac{K_f}{M} z_3 - \frac{k(z_2z_3 + A_b z_2 z_4/M + K_f z_2^2/M)}{l/2 + z_1 + \Delta} + \frac{kRT_s C_d C_0 w_a \hat{f}(z, P_s, P_e)}{M(l/2 + z_1 + \Delta)} u_1 \\ &\quad - \frac{kz_4z_2}{l/2 - z_1 + \Delta} - \frac{kRT_s C_d C_0 w_b \hat{f}(z_4, P_s, P_e)}{A_b(l/2 - z_1 + \Delta)} u_2, \\ \dot{z}_4 &= \frac{kz_4z_2}{l/2 - z_1 + \Delta} + \frac{kRT_s C_d C_0 w_b \hat{f}(z_4, P_s, P_e)}{A_b(l/2 - z_1 + \Delta)} u_2. \end{aligned} \quad (11)$$

Let

$$u_1 = \frac{M(l/2 + z_1 + \Delta)}{kRT_s C_d C_0 w_a \hat{f}(z, P_s, P_e)} \left[\frac{k(z_2 z_3 + A_b z_2 z_4 / M + K_f z_2^2 / M)}{l/2 + z_1 + \Delta} - qz_4 + V_1 \right],$$

$$u_2 = \frac{l/2 - z_1 + \Delta}{kRT_s C_d C_0 w_b \hat{f}(z_4, P_s, P_e)} \left[\frac{-kz_2 z_4}{l/2 - z_1 + \Delta} - qz_4 + V_2 \right],$$

where q is a design parameter with a positive real value. Substituting u_1 and u_2 back into (11), we have

$$\begin{aligned} \dot{z}_1 &= z_2, \\ \dot{z}_2 &= z_3, \\ \dot{z}_3 &= -\frac{K_f}{M} z_3 + V_1 - V_2, \\ \dot{z}_4 &= -qz_4 + V_2, \\ y &= z_1. \end{aligned} \tag{12}$$

So system (12) is linear with two independent inputs V_1 and V_2 , and its input–output map is obviously also linear.

4. TRACKING CONTROL DESIGN

Similarly, the discussion starts from the case of using a single five-port valve. Linearized subsystem (10a) can be rewritten in a matrix form as follows:

$$\dot{\bar{z}} = A_1 \bar{z} + B_1 V, \tag{13}$$

$$\text{where } \bar{z} = \begin{bmatrix} z_1 \\ z_2 \\ z_3 \end{bmatrix}, A_1 = \begin{bmatrix} 0 & 1 & 0 \\ 0 & 0 & 1 \\ 0 & 0 & -\frac{K_f}{M} \end{bmatrix}, \text{ and } B_1 = \begin{bmatrix} 0 \\ 0 \\ 1 \end{bmatrix}.$$

For a tracking problem, suppose that it requires the system output z_1 to follow the trajectory $\theta_1(t)$ accurately. As (A_1, B_1) is a controllable pair, $\theta_1(t)$ can be normally generated by the linear system of the same structure as (13). Let $\theta = [\theta_1 \ \theta_2 \ \theta_3]^T$. We have

$$\begin{bmatrix} \dot{\theta}_1 \\ \dot{\theta}_2 \\ \dot{\theta}_3 \end{bmatrix} = \begin{bmatrix} 0 & 1 & 0 \\ 0 & 0 & 1 \\ 0 & 0 & -\frac{K_f}{M} \end{bmatrix} \begin{bmatrix} \theta_1 \\ \theta_2 \\ \theta_3 \end{bmatrix} + \begin{bmatrix} 0 \\ 0 \\ 1 \end{bmatrix} \omega(t), \quad (14)$$

where $\omega(t)$ is an external input which will be designed to generate the desired trajectory $\theta_1(t)$. With (14), the tracking problem can be converted into an asymptotical stability problem. Let $e(t) = \theta(t) - \bar{z}(t)$. Then we have

$$\dot{e} = \dot{\theta} - \dot{\bar{z}} = A_1(\theta - \bar{z}) + B_1(V - \omega) = A_1e + B_1(V - \omega). \quad (15)$$

A feedback controller can be developed to drive the error state $e(t)$ to zero. The controller can be chosen to have the structure

$$V = -Ke + \omega,$$

where $K = [K_1 \ K_2 \ K_3]$. The closed-loop system is then written as $\dot{e} = (A_1 - B_1K)e$.

If the feedback control can be designed to guarantee that $\sigma(A_1 - B_1K) \in C^-$, the tracking error $e(t)$ will eventually approach to zero within a finite time period.

Substitute the tracking control V back to the original system control u . The following is obtained:

$$u = \frac{k(z_2z_3 + K_f z_2^2/M)}{\psi(z)(l/2 + z_1 + \Delta)} + \frac{A_b k(l + 2\Delta)z_2z_4}{\psi(z)[(l/2 + \Delta)^2 - z_1^2]} + \frac{1}{\psi(z)}[K_1(\theta_1 - z_1) + K_2(\theta_2 - z_2) + K_3(\theta_3 - z_3) + \omega]. \quad (16)$$

By substituting $z = Tx$ into (16) the final feedback control $u(x)$ can be derived straightforwardly.

For the case of using two three-port valves, the system is linearized as shown in (12). The feedback control can be designed in two stages, that is, starting from V_2 to V_1 . Let $V_2 = -K_4z_4$. If the design parameter q has been properly chosen, V_2 may be simply set to zero ($V_2 = 0$). In this case, (12) would be identical to (10a), which implies that the same feedback control design procedure can be applied to this case. Therefore, the controller with respect to the state variables z is as follows:

$$u_1 = \frac{Mz_2z_3 + A_bz_2z_4 + K_fz_2^2}{RT_sC_dC_0w_a\hat{f}(z, P_s, P_e)} - \frac{M(l/2 + z_1 + \Delta)(qz_4 + \omega)}{kRT_sC_dC_0w_a\hat{f}(z, P_s, P_e)} - \frac{[K_1(\theta_1 - z_1) + K_2(\theta_2 - z_2) + K_3(\theta_3 - z_3)]}{1/[M(l/2 + z_1 + \Delta)]kRT_sC_dC_0w_a\hat{f}(z, P_s, P_e)}, \quad (17)$$

$$u_2 = \frac{l/2 - z_1 + \Delta}{kRT_sC_dC_0w_b\hat{f}(z_4, P_s, P_e)} \left[\frac{-kz_2z_4}{l/2 - z_1 + \Delta} - qz_4 \right]. \quad (18)$$

Similarly, by substituting $z = Tx$ into u_1 and u_2 the final feedback control $u_1(x)$ and $u_2(x)$ will be derived for the second case.

5. SIMPLIFIED TRACKING CONTROL AND SIMULATION STUDY

The tracking controls (16)–(18) might be too complicated for real-time implementation. It is desired to simplify the feedback tracking control for practical applications. The analysis of the characteristics of function \hat{f} shows that the value of the function is between (0, 1] and the average is around 0.75. If \hat{f} is chosen to be replaced by 0.75, the controller designed in Section 4 can be much simpler. Similarly, $0.75P_s/\sqrt{T_s}$ is, in turn, used to approximate \hat{f} . The approximation process is described in the following subsections.

Case I. Using a single five-port valve

Let $\tilde{C} = \frac{1}{0.75P_sR\sqrt{T_s}C_dC_0w(l+2\Delta)}$. Then

$$u = \tilde{C}x_2[A_ax_3(l/2 + \Delta - x_1) + A_bx_4(l/2 + \Delta + x_1)] + \tilde{C}M[(l/2 + \Delta)^2 - x_1^2] [-Ke + \omega]/k. \quad (19)$$

Note that all the terms in \tilde{C} are constants. So the controller is much simpler than the original control structure shown in (16).

Case II. Using two three-port valves

Let $\tilde{C}_1 = \frac{1}{0.75P_s kR\sqrt{T_s}C_dC_0w_a}$ and $\tilde{C}_2 = \frac{1}{0.75P_s kR\sqrt{T_s}C_dC_0w_b}$. Then we have

$$u_1 = \tilde{C}_1[kx_2x_3 - M(l/2 + \Delta + x_1)qx_4 - M(l/2 + \Delta + x_1)(Ke - \omega)], \quad (20)$$

$$u_2 = \tilde{C}_2[-kx_2x_4 - q(l/2 + \Delta - x_1)x_4]. \quad (21)$$

Again, the simplified versions (20) and (21) are simpler than (17) and (18).

However, it is unknown if the controllers (19) and (20)–(21) can guarantee a satisfactory tracking precision. Simulation studies are carried out to compare the tracking accuracy of using (16) with the results of using (19). The conditions specified for the simulations are: rodless cylinder, cylinder bore size $\phi = 0.32$ m; cylinder length $l = 1$ m; compressed air supply pressure $P_s = 6 \times 10^5$ N/m²; initial position $x = -0.5$ m; initial velocity $\dot{x} = 0$ m/s; initial chamber pressures $P_a = 4.5 \times 10^5$ N/m²; and $P_b = 4.2 \times 10^5$ N/m²; $K_S = 0$; $K_C = 0$; and $K_f = 15$ Ns/m. The desired tracking trajectory can be described as $\theta_1(t) = -0.5 \cos(0.5\pi t)$, for $0 \leq t \leq 2$. The simulation results using the controllers (16) and (19) are shown in Figs 2 and 3, respectively. Here, it is necessary to point out that the simulation is

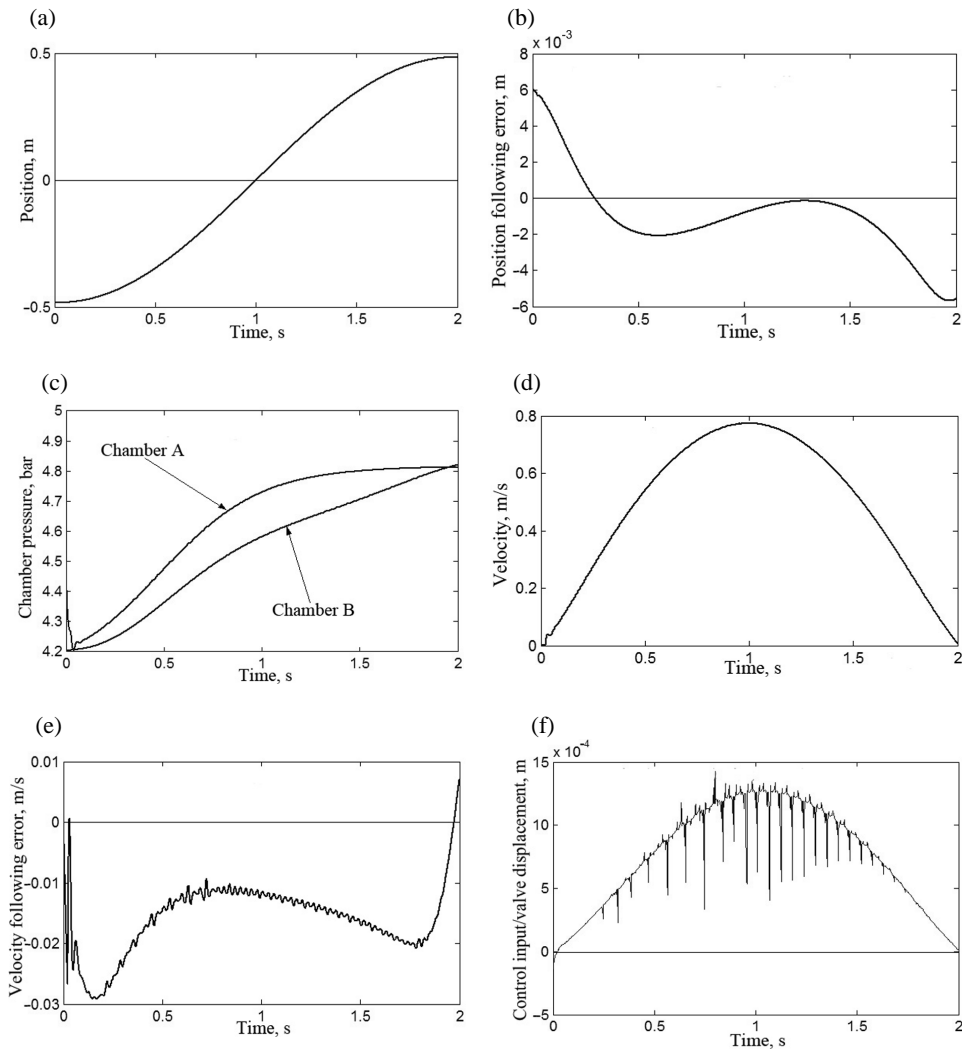


Fig. 2. Simulation results using the feedback tracking control described in (17): (a) position; (b) position following error; (c) chamber pressures; (d) velocity; (e) velocity following error; (f) control input.

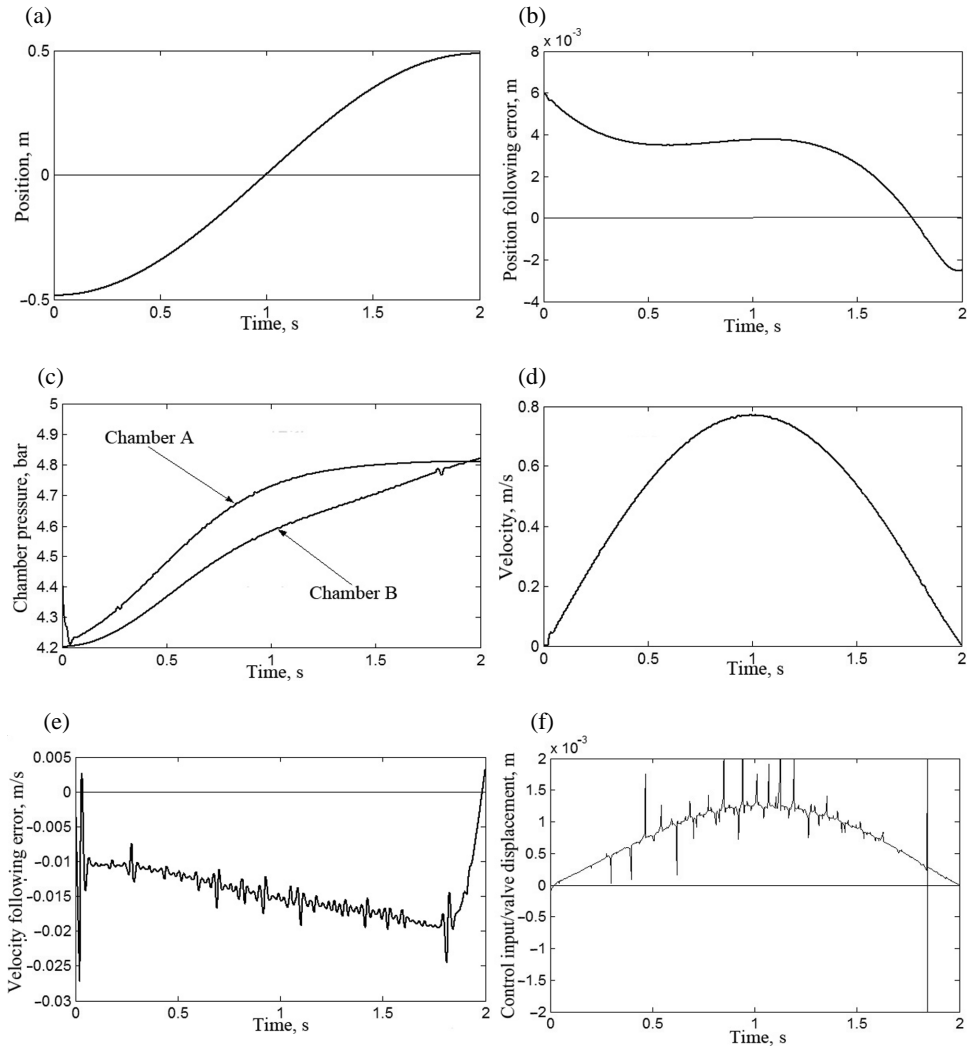


Fig. 3. Simulation results using the simplified feedback tracking control described in (20): (a) position; (b) position following error; (c) chamber pressures; (d) velocity; (e) velocity following error; (f) control input.

conducted for the case of using a single five-port valve, because it is adopted in a wider range of practical applications.

From Figs 2 and 3 it can be seen that the approximated feedback control has a similar position tracking accuracy, that is, the maximum error is less than 6 mm or the relative error is less than 0.6%. But the velocity responses and the feedback control input are more violent when using the approximated feedback controller. In practice, the choice of the feedback control must compromise the

tracking accuracy, smoothness of responses, and the complexity of the controller structure.

Both controllers described in (16) and (19) use full state feedback, which means that it is required to measure the position, velocity, and two chamber pressures. To get all this information, at least three sensors are needed – position (velocity), chamber A pressure, and chamber B pressure sensors. Generally, using three sensors in the system is not cost-effective for many industrial applications. Therefore, it is desired to simplify the controller structure further to not include the chamber pressures in state feedback. A test has been conducted to replace the chamber pressure variables by constants. In this test, the pressures x_3 and x_4 are replaced by μP_s and ηP_s , and also, the feedback parameter $K_3 = 0$. Then

$$u = \tilde{C}x_2[A_a\mu P_s(l/2 + \Delta - x_1) + A_b\eta P_s(l/2 + \Delta + x_1)] + \tilde{C}M[(l/2 + \Delta)^2 - x_1^2][-Ke + \omega]/k. \quad (22)$$

As the test uses a rodless cylinder, $A_a = A_b = A$. Then

$$u = \tilde{C}x_2A[(\mu + \eta)(l/2 + \Delta) - (\mu - \eta)x_1] + \tilde{C}M[(l/2 + \Delta)^2 - x_1^2][-Ke + \omega]/k. \quad (23)$$

Generally, $(\mu - \eta)x_1$ is much smaller than $(\mu + \eta)(l/2 + \Delta)$. Therefore, (23) may be further simplified to

$$u = \tilde{C}x_2A(\alpha + \beta)(l/2 + \Delta) + \tilde{C}M[(l/2 + \Delta)^2][-Ke + \omega]/k - \tilde{C}Mx_1^2[-Ke + \omega]/k. \quad (24)$$

Using \hat{K}_i to replace the coefficients in (24), the feedback tracking control law can be rewritten in the following form:

$$u = \hat{K}_1x_2 + \hat{K}_2[-Ke + \omega] - \hat{K}_3x_1^2[-Ke + \omega],$$

where $\hat{K}_1 = \tilde{C}x_2A(\alpha + \beta)(l/2 + \Delta)$, $\hat{K}_2 = \tilde{C}M[(l/2 + \Delta)^2]/k$, and $\hat{K}_3 = \tilde{C}M/k$. The controller shown in (24) is simple enough to be implemented in real-time control. The simulation results are shown in Fig. 4.

From the above simulation results, the tracking accuracy is within ± 9 mm, which is acceptable in comparison with the results obtained using the nonlinear feedback in (16) but the dynamic responses are much more violent. If this approximated feedback control is chosen, the necessary filters need to be introduced to get smooth responses before it can be applied to the system. With $K_3 = 0$, the first two terms of the controller (24) can be considered as a nonlinear PI control combined with the velocity feedback.

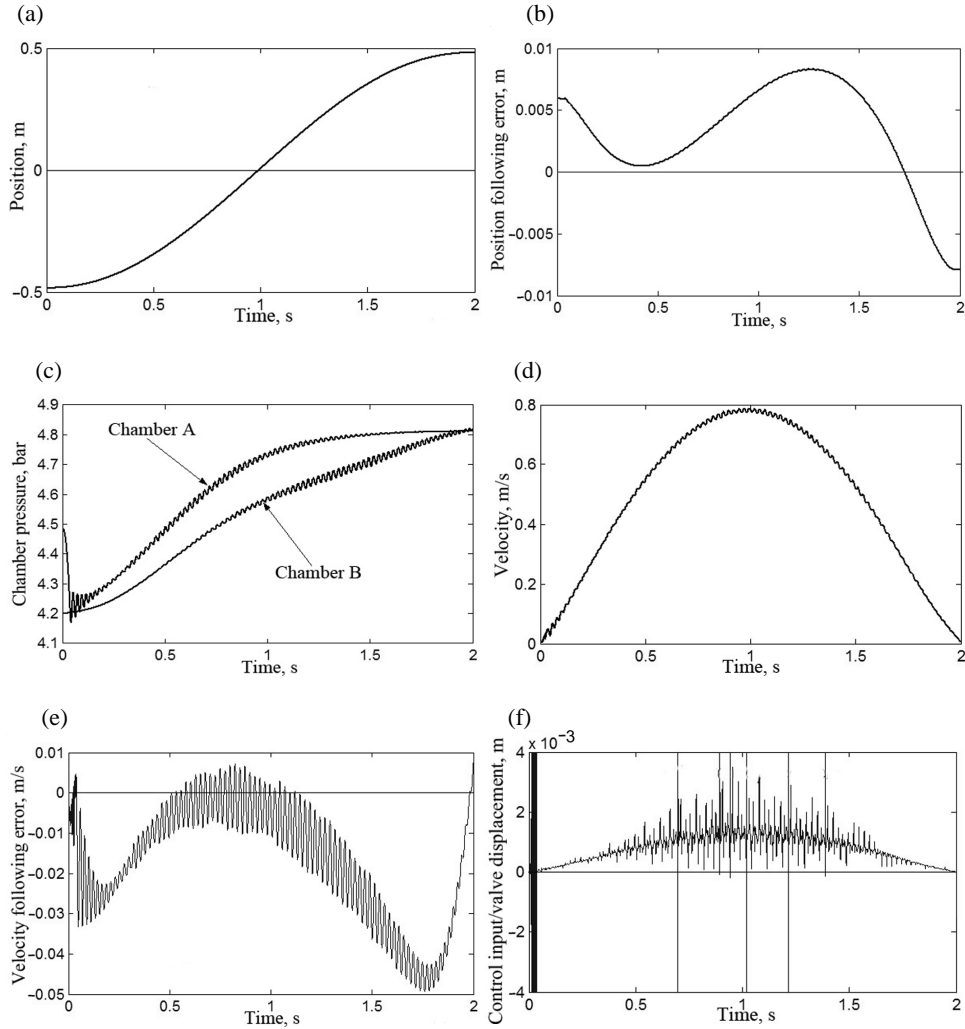


Fig. 4. Simulation results using the further simplified feedback tracking control described in (25): (a) position; (b) position following error; (c) chamber pressures; (d) velocity; (e) velocity following error; (f) control input.

6. FEEDBACK CONTROL DESIGN FOR THE SYSTEM WITH UNKNOWN FRICTIONS

In Sections 4 and 5, the combined friction force $K_{S-c}(x_1)S(x_2, x_3, x_4)$ and the load variation effects are neglected for the convenience of analysis. When the system has the combined static and dynamic frictions, a simulation is conducted with $F_C = 20$ N, $F_S = 30$ N, using the feedback controller (16). The simulation results are shown in Fig. 5.

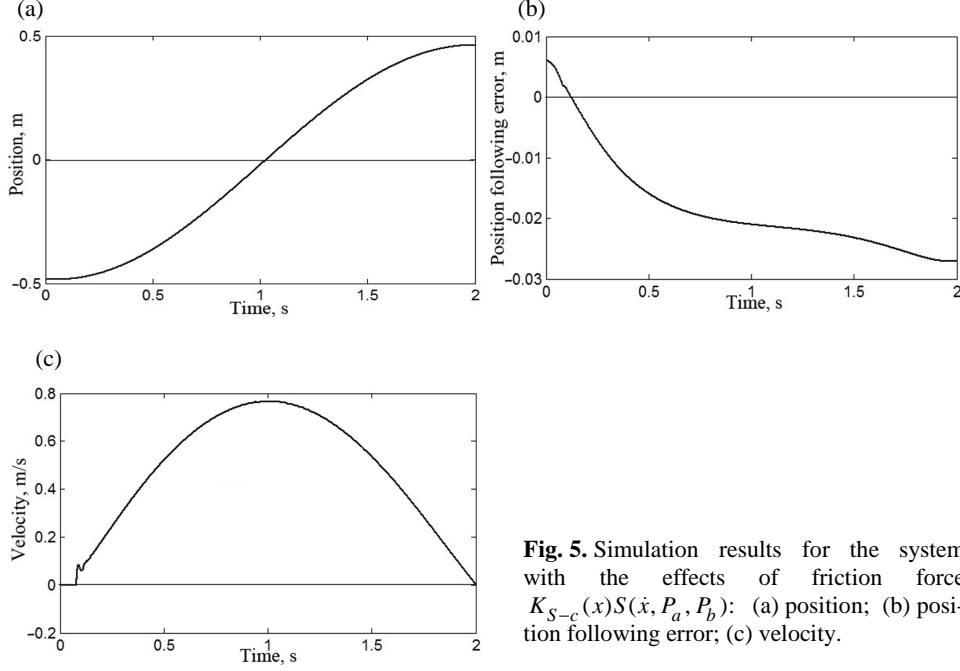


Fig. 5. Simulation results for the system with the effects of friction force $K_{S-c}(x)S(\dot{x}, P_a, P_b)$: (a) position; (b) position following error; (c) velocity.

In Fig. 5, it can be seen that the tracking error is over 2.5% and there is obvious time-delay in velocity responses while the influences of friction forces are considered. In practice, the static friction of a cylinder has an uneven distribution along the cylinder and varies with the environment changes [17]. Therefore, it is necessary to develop a control strategy to address the uncertain frictions and the load effects. From the practical point of view, an efficient way to overcome the static friction to lead the pneumatic system to have a fast starting response is to open the control valve fully and give the maximum compressed air flow rate at the initial stage of the piston movement. As previous simulation and experiment study has shown [12], this method is simple but effective. A similar method is used in this paper, combined with the tracking control strategy described in Section 5.

From Eq. (1b), $\dot{x}_2 = 1/M [-K_f x_2 - K_{S-c}(x_1)S(x_2, x_3, x_4) + A_a x_3 - A_b x_4]$. When the piston starts moving, the static friction force is zero and only the F_C term is left in $K_{S-c}S(x_2, x_3, x_4)$. Equation (1b) becomes $\dot{x}_2 = 1/M [-K_f x_2 - F_C + A_a x_3 - A_b x_4]$, in which \dot{x}_2 represents the acceleration of the piston. Due to the effect of F_C , the resulting acceleration by the force $A_a x_3 - A_b x_4$ will be reduced. If we can estimate the decreases in acceleration, the friction force F_C can be roughly obtained. Based on this idea, a friction compensation control strategy is proposed. There are two key aspects of the control strategy.

1. To reduce the time-delay caused by static friction: When the piston velocity is zero and $A_a x_3 - A_b x_4$ is less than F_S , the piston stands still. During this period, the valve is set to fully open, that is, u is set to have the maximum

positive/negative valve displacement, which will replace the tracking control described by (16) or (17)–(18) or (19) or (20)–(21) or (24).

2. To reduce the tracking errors caused by the friction term or variable load of F_C : Suppose that the friction force $F_C = 0$. Then the estimated acceleration would be $\hat{a} = 1/M[-K_f x_2 + A_a x_3 - A_b x_4]$. In fact, the acceleration of the piston is measured assuming that it will be represented by \tilde{a} . The relative difference between the measured and estimated acceleration values can be calculated by $a_{er} = (\tilde{a} - \hat{a})/\hat{a}$. This difference will be used to amend the tracking control law. The amendment of the tracking control law should also use the information of the position tracking error, that is, the difference of the desired and measured positions, e_1 . The proposed update tracking control law is $u^* = u(1 + \kappa a_{er}(e_1/x_{1max}))$, where u is the tracking control law obtained through (16) or (17)–(18) or (19) or (20)–(21) or (24), x_{1max} is the absolute value of the maximum piston position, and κ is a parameter of the updating rate, which will be determined through the simulation or experiment test.

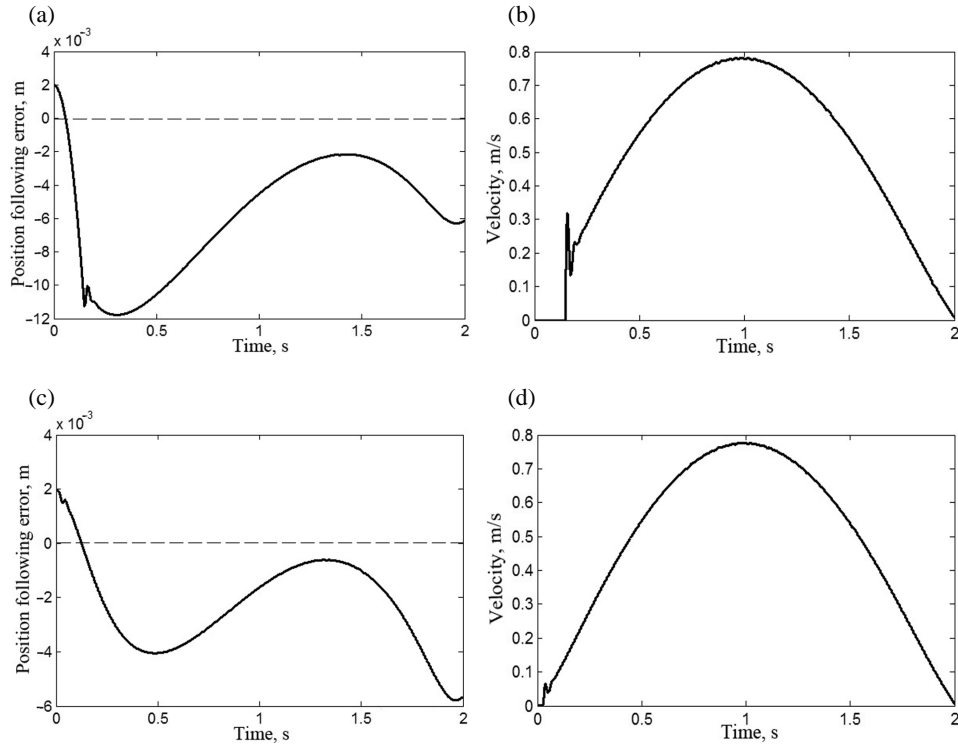


Fig. 6. Simulation results for the system with the static friction force $F_S = 45$ N: (a),(b) simulation results using the control strategy described by (17); (c),(d) simulation results using the enhanced control strategy to address the static frictions.

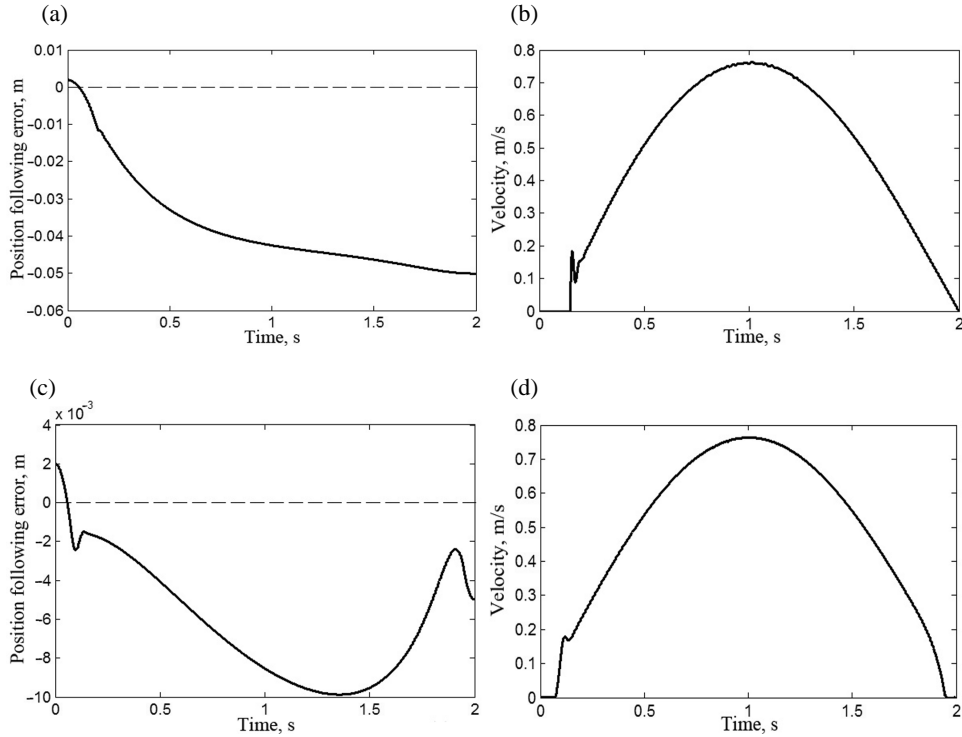


Fig. 7. Simulation results for the system with the static friction force $F_C = 20$ N and $F_S = 45$ N: (a),(b) simulation results using the control strategy described by (17); (c),(d) simulation results using the enhanced control strategy to address the frictions.

Using the same pneumatic cylinder system as described in Section 5 and adopting the tracking control strategy proposed in this section, the simulation results are shown below, in which $x_{1\max} = 0.5$ m and κ is chosen to have the value of 100. The results of the simulation with adopting the tracking control law u described in (16) are shown in Fig. 6.

Figures 6 and 7 show that the time-delay in the velocity responses and the position tracking errors are reduced dramatically when the enhanced control strategy is applied to address the problems caused by the friction forces.

7. CONCLUSIONS

Nonlinear pneumatic actuator systems are linearized via input–output feedback linearization. Based on the linearized model, a feedback tracking control is proposed using the well-developed linear control theory. Then the feedback control is transformed back to the nonlinear state space. For convenience, the static friction is ignored initially and treated as uncertainties in later analysis. The nonlinear feedback control is simplified for the purpose of real-time implementa-

tion. The simulation results show that the simplified control offers satisfactory tracking accuracy. To address the problems caused by the friction forces, an enhanced tracking control strategy is proposed, based on a simple idea of comparing the measured acceleration with the estimated acceleration under the conditions without friction influences. The estimated value is then used to amend the control strategy proposed for the situation when the friction forces are ignored. The main advantage of the method proposed in the paper is that it has a clear theoretic guidance at the initial stage of controller design and leads to a simpler tracking control strategy.

ACKNOWLEDGEMENT

Ü. Kotta would like to thank the Estonian Science Foundation (grant No. 6922) for financial support.

REFERENCES

1. Conte, C., Moog, C. H. and Perdon, A. M. Nonlinear control systems. *Lecture Notes in Control and Inform. Sci.*, 1999, 242, Springer-Verlag, London.
2. Isidori, A. *Nonlinear Control Systems*, 3rd Edition. Springer-Verlag, London, 1995.
3. Jiang, L., Wu, Q. H., Wang, J., Zhang, C. and Zhou, X. X. Robust observer-based nonlinear control of multi-machine power systems, *IEE Proc. Power Gener. Distrib.*, 2001, **148**, 623–631.
4. Hahn, K. Selecting a linear motion control technology. *Control Solutions*, 2001, 12–16.
5. Ben-Dov, D. and Salcudean, S. E. A force-controlled pneumatic actuator. *IEEE Trans. Robot. Autom.*, 1993, **11**, 906–911.
6. Drakunov, S., Hanchin, G. D., Su, W. C. and Ozguner, U. Nonlinear control of a rodless pneumatic servoactuator, or sliding modes versus Coulomb friction. *Automatica*, 1997, **33**, 1401–1408.
7. McDonnell, B. W. and Bobrow, J. E. Adaptive tracking control of an air powered robot actuator. *ASME J. Dynam. Systems, Measurement, Control*, 1993, **115**, 427–433.
8. Moore, P. R., Pu, J. and Harrison, R. Progression of servo pneumatics towards advanced applications, In *Fluid Power Circuit, Component and System Design* (Edge, K. and Burrows, C., eds). Research Studies Press, 1993, 347–365.
9. Sesmat, S., Scavarda, S. and Lin-shi, X. Verification of electropneumatic servovalve size using non-linear control theory applied to cylinder position tracking, In *The Proceedings of the 4th Scandinavian International Conference on Fluid Power*. Tampere, Finland, 1995, **1**, 504–511.
10. Van Varseveld, R. B. and Bone, G. M. Accurate position control of a pneumatic actuator using on/off solenoid valves. *IEEE/ASME Trans. Mechatronics*, 1997, **2**, 195–204.
11. Wang, J., Pu, J., Moore, P. R. and Zhang, Z. Modeling study and servo-control of air motor systems. *Int. J. Control*, 1998, **71**, 459–476.
12. Wang, J., Pu, J. and Moore, P. R. A practicable control strategy for servo pneumatic actuator systems. *Control Eng. Pract.*, 1999, **7**, 1483–1488.
13. Wang, J., Kotta, Ü., Mangan, S. and Wei, J. Robust tracking control of nonlinear pneumatic systems using input/output linearisation by state feedback. *Syst. Sci.*, 2003, **29**, 151–165.
14. Anderson, B. W. *The Analysis and Design of Pneumatic Systems*. Robert E. Krieger Publishing Co., INC, New York, 1976.

15. Armstrong-Helouvry, S., Dupont, P. and Canudas De Wit, C. A survey of model, analysis tool and compensation methods for the control of machines with friction. *Automatica*, 1994, **30**, 1083–1183.
16. Blackburn, J. F., Reethof, G. and Shearer, J. L. *Fluid Power Control*. The Technology Press and J. Wiley Inc., New York, 1960.
17. Wang, J., Wang, D. J. D., Moore, P. R. and Pu, J. Modeling study, analysis and robust servo control of pneumatic cylinder actuator systems. *IEE Proc. Control Theory Appl.*, 2001, **148**, 35–42.

Mittelineaarse pneumaatilise süsteemi juhtimine tema mudeli sisend-väljundkujutise lineariseerimise kaudu

Jihong Wang, Ülle Kotta ja Jia Ke

On esitatud juhtimisstrateegia pneumaatilise süsteemi juhtimiseks eesmärgiga saavutada kolvi etteantud trajektoori järgimisel suurem täpsus. Meetod põhineb pneumaatilise süsteemi mittelineaarse mudeli tagasisidega lineariseerimisel. Kasutades staatilist mittelineaarset olekutagasisidet ja koordinaatteisendust olekute ruumis, on süsteem teisendatud kujule, millel on lineaarne sisend-väljundkujutis ja lihtne lineaarne alamsüsteem olekute ruumis. Seejärel on juhttoime leidmiseks võimalik kasutada lineaarsete juhtimissüsteemide teoriast tuntud algoritme. Et mittelineaarsetel teisendustel eksisteerivad pöördteisendused, on esitatud lineaarse teooria põhjal leitud juhtimisalgoritmid süsteemi esialgsete olekukoordinaatide ja juhttoimete kaudu. Artiklis on käsitletud kaht juhtu: pneumaatilist silindrit juhitakse vastavalt kas ühe või kahe klapiga. Juhttoime esialgsel leidmisel ignoreeritakse hõõrdejõude, need tuuakse hiljem sisse kui süsteemi olekute häiringud. Kontrolleri praktiliseks rakendamiseks tuleb leitud juhttoimet lihtsustada aproksimeerimise teel nii, et tagasiside sõltuks ainult kolvi asendist ja kiirusest. Simuleerimistulemused näitavad, et lihtsustatud kontroller kindlustab etteantud trajektoori järgimisel nõutava täpsuse.